A Novel Motion Equation for General Task Description and Analysis of Mobile-Hapto

Article *in* IEEE Transactions on Industrial Electronics · July 2013

DOI: 10.1109/TIE.2012.2196009

Sho Sakaino
University of Tsukuba

A Novel Motion Equation for General Task Description and Analysis of Mobile-Hapto

Sho Sakaino, *Member, IEEE*, Tomoya Sato, *Student Member, IEEE*, and Kouhei Ohnishi, *Fellow, IEEE*

***Abstract*—In this paper, mobile-hapto is analyzed, which is a remote control system that enables the realization of two tasks: velocity control of a mobile robot and force transmission between a handle robot and a mobile robot. To date, there have been no analyses of mobile-hapto because of the fact that the dynamics of mobile-hapto is difficult to derive without the motion equation proposed in our previous study. This motion equation, in turn, allowed for the proposal of a stable mobile-hapto controller. In this paper, the proposed mobile-hapto controller is analytically compared to a conventional mobile-hapto controller. The results show that decoupled tasks can be obtained only in the proposed method. We also show the robustness of the proposed method. To confirm the validity of the proposed method, the proposed controller is experimentally compared to the conventional controller. This is the foremost study on the analysis and experimental comparison of mobile-hapto. Consequently, the usefulness of the proposed motion equation is shown.**

***Index Terms*—Bilateral control, haptics, mobile-hapto, motion equation, port-controlled Hamiltonian system.**

I. Introduction

RECENTLY, many researchers are studying robot engineering as the social foundation of the next generation. The use of robots is changing and expanding, for example, in the field of medical care, welfare, and entertainment. These robots are very different from the conventional manufacturing robots in the way that they support human activities. Because there are many unknown obstacles and disturbances in human environments, robot systems tend to be unstable in conventional robot controllers. In addition, because human motion is composed of various tasks with many degrees of freedom (DOFs), a way to describe tasks involving human motion is essential. Therefore, there are two requirements in this study: robust controllers and a description of tasks.

A famous controller to realize robust control systems is a disturbance observer (DOB) [1]. Disturbances are suppressed by acceleration feedback responses of robots. Acceleration control based on the DOB is effective to increase robustness to modeling errors and uncertain environments. Many useful extensions of the DOB show its effectiveness [2]–[4]. The kinematic errors can be compensated by an operational space DOB [5]. Time-delayed systems are stabilized by a communication DOB [6]. Yi *et al.* showed that hysteresis characteristics could be compensated by the DOB [7]. Some researchers show that sliding-mode controllers are effective to increase the performance of the DOB [8]–[10]. The DOB improves the performance of not only position-controlled systems but also force-controlled systems [11].

Descriptions of tasks have also been studied [12], [13]. Tsuji *et al.* showed a basic solution to describe tasks, defined as "functionality," by exploiting the DOB. Functionality is given by coordinate transform, defined as "modal transform" [14]. Tsuji *et al.* insist that tasks should be described by coordinate transform and a combination of tasks can be given by a combination of coordinate transform matrices. However, their methods must be applied with two strong constrained conditions. First, robots should have a single DOF, and second, the mass of robots should be equal; otherwise, tasks are difficult to realize owing to interferences of the robots with themselves. Sabanovic *et al.* investigated modal transform with a sliding-mode controller [15]; however, they can only treat tasks related to position. Recently, Sakaino *et al.* showed that functionality is equivalent to position/force hybrid control problems [16]. Because the interferences of tasks can be described by off-diagonal parameters of mass matrices in position/force hybrid control, which is well known among robot engineers [17]–[19], tasks are decoupled without requiring the aforementioned two conditions. Owing to this characteristic, designers need not worry about the interferences and can concentrate on finding appropriate coordinate systems (tasks). Once an appropriate coordinate system is found, it can be applied to other systems without considering interferences. In other words, tasks are used as reusable components. Even though a system is complicated and large, the system can be treated as a combination of small tasks that impose fewer restrictions on designers.

All of the controllers previously mentioned are derived from the Lagrange equation, which describes coordinate transform with functions of position or time. In general, there are tasks that are given by coordinate transform including velocity (e.g., velocity limitation). Therefore, the exact description of task dynamics including velocity is difficult to explain, and it requires many assumptions that are sometimes not explicitly mentioned for implementation.

The canonical equation is a well-known extension of the Lagrange equation treating coordinate transform described by

Manuscript received February 22, 2011; revised November 9, 2011 and February 29, 2012; accepted April 6, 2012. Date of publication April 26, 2012; date of current version February 28, 2013.

S. Sakaino is with Sakaino Laboratory, Department of Electrical and Electronic Systems, Saitama University, Saitama 338-8570, Japan (e-mail: sakaino@mail.saitama-u.ac.jp).

T. Sato and K. Ohnishi are with Ohnishi Laboratory, Department of System Design Engineering, Keio University, Yokohama 223-8522, Japan (e-mail: sat@sum.sd.keio.ac.jp; ohnishi@sd.keio.ac.jp).

Color versions of one or more of the figures in this paper are available online at http://ieeexplore.ieee.org.

Digital Object Identifier 10.1109/TIE.2012.2196009

functions of position, momentum, or time. There are, however, three disadvantages. First, coordinate transform of external forces is not provided. It is a critical assumption for robot control because control inputs are usually described as external forces. Second, coordinate transform is not arbitrarily realized. Third, solving partial differential equations is necessary.

Fujimoto and Sugie recently proposed a generalized canonical transform that overcame the aforementioned disadvantages [20], [21]. They described the dynamics in port-controlled Hamiltonian systems [22], [23]. However, when a coordinate transform function includes time (e.g., trajectory servo problems), partial differential equations need to be solved [24], [25].

In the previous study, we proposed a novel motion equation to solve the aforementioned three problems [26]. The problem of a generalized canonical transform is easily solved by treating time as generalized position in the extended phase space. In the proposed equation, coordinate transform may be functions of any physical parameter. In addition, the transform is algebraically supplied without any conditions or solving of differential equations. Furthermore, the transform is applicable to external forces. We proposed a mobile-hapto controller as an example of the proposed motion equation. The concept of mobile-hapto was originally proposed by Yamanouchi *et al.* [27]. Mobile-hapto is a remote control system requiring two tasks. First, the velocity of a remote mobile robot is controlled by the inclination of a local handle robot. Second, the reaction force of the mobile robot is fed back to the handle robot. Because the first task includes the velocity, only the proposed motion equation can treat mobile-hapto as coordinate transform.

In the previous study, the proposed mobile-hapto controller [26] was shown to be superior to the conventional mobile-hapto controller [27]. In this paper, the conventional and proposed methods are analyzed to show the effectiveness. We will first reveal that there are interferences of tasks in the conventional method. In the proposed method, each task is decoupled because the dynamics of the tasks are given by coordinate transform. Second, we will reveal the robustness of the proposed method by showing that there is no relation between the stability of the proposed system and a modeling error of the mass of the handle robot. The validity of the proposed method is experimentally verified. Note that the analysis of mobile-hapto and the derivation of the proposed controller are obtained only by using the proposed motion equation. Without the proposed motion equation, the dynamics of mobile-hapto systems are still covered. For this reason, we can show the usefulness of the proposed motion equation.

This paper is composed of six parts, including this section. In Section II, the proposed motion equation is shown. The dynamics and controller of mobile-hapto are derived in Section III. The proposed method is analytically compared to the conventional method in Section IV. In Section V, experimental results are shown. This paper is summarized in Section VI.

II. System Description

The variables and the proposed motion equation are shown in this section.

A. Variables

In this paper, $\boldsymbol{I}_n$ and $\boldsymbol{0}_n$ are an n-dimensional unit matrix and an n-dimensional zero matrix, respectively. $\boldsymbol{q}$ and $\boldsymbol{p}$, where $\boldsymbol{q} = (q_1, q_2, \ldots, q_n)^{\mathrm{T}}$ and $\boldsymbol{p} = (p_1, p_2, \ldots, p_n)^{\mathrm{T}}$, are described as n-dimensional generalized position and momentum, respectively. Designator n is a number of DOF of systems. H is the Hamiltonian, which satisfies the next relation

$$H(\boldsymbol{q}, \boldsymbol{p}, t) = \boldsymbol{p}^{\mathrm{T}}\dot{\boldsymbol{q}} - L(\boldsymbol{q}, \dot{\boldsymbol{q}}, t). \tag{1}$$

This is the Legendre transformation from the Lagrangian $L(\boldsymbol{q}, \dot{\boldsymbol{q}}, t)$ to $H(\boldsymbol{q}, \boldsymbol{p}, t)$.

In the extended phase space, time is treated as position, and the Hamiltonian is momentum as dual basis of time

$$\hat{\boldsymbol{q}} = (\hat{q}_0, \hat{q}_1, \ldots, \hat{q}_n)^{\mathrm{T}} = \left(t, \boldsymbol{q}^{\mathrm{T}}\right)^{\mathrm{T}} \tag{2}$$

$$\hat{\boldsymbol{p}} = (\hat{p}_0, \hat{p}_1, \ldots, \hat{p}_n)^{\mathrm{T}} = \left(-H, \boldsymbol{p}^{\mathrm{T}}\right)^{\mathrm{T}} \tag{3}$$

$$\hat{H}(\hat{\boldsymbol{q}}, \hat{\boldsymbol{p}}) = \hat{H}(\boldsymbol{q}, \boldsymbol{p}, t, \hat{p}_0) = H(\boldsymbol{q}, \boldsymbol{p}, t) + \hat{p}_0 = 0. \tag{4}$$

Therefore, in this space, an energy-like term $\hat{H}(\hat{\boldsymbol{q}}, \hat{\boldsymbol{p}})$ is conservative.

B. Motion Equation

A general motion equation is shown here. This equation found using the extended phase space is a good solution to realize general coordinate transform. The following equation is the motion equation:

$$\dot{\boldsymbol{x}} = \boldsymbol{J}(\boldsymbol{x})\frac{\partial \hat{H}(\boldsymbol{x})}{\partial \boldsymbol{x}}^{\mathrm{T}} + \boldsymbol{u}. \tag{5}$$

Here, $\boldsymbol{x}$ is a phase variable, $\boldsymbol{J}$ is a skew symmetric matrix, and $\boldsymbol{u}$ is the effect of external forces

$$\boldsymbol{x} = \left(\hat{\boldsymbol{q}}^{\mathrm{T}}, \hat{\boldsymbol{p}}^{\mathrm{T}}\right)^{\mathrm{T}} \tag{6}$$

$$\boldsymbol{J}(\boldsymbol{x}) = \begin{bmatrix} \boldsymbol{0}_{n+1} & \boldsymbol{I}_{n+1} \\ -\boldsymbol{I}_{n+1} & \boldsymbol{0}_{n+1} \end{bmatrix}. \tag{7}$$

By using this motion equation, general (arbitrary) coordinate transform is described as follows:

$$\overline{\boldsymbol{x}} = \begin{pmatrix} \hat{\boldsymbol{Q}} \\ \hat{\boldsymbol{P}} \end{pmatrix} = \boldsymbol{\Phi}(\boldsymbol{x}). \tag{8}$$

Variables $\boldsymbol{Q}$, $\hat{\boldsymbol{Q}}$, $\boldsymbol{P}$, $\hat{\boldsymbol{P}}$, and K are a generalized position, generalized momentum, and the Hamiltonian after transformation, respectively

$$\hat{\boldsymbol{Q}} = (\hat{Q}_0, \hat{Q}_1, \ldots, \hat{Q}_n)^{\mathrm{T}} = \left(t, \boldsymbol{Q}^{\mathrm{T}}\right)^{\mathrm{T}} \tag{9}$$

$$\hat{\boldsymbol{P}} = (\hat{P}_0, \hat{P}_1, \ldots, \hat{P}_n)^{\mathrm{T}} = \left(-K, \boldsymbol{P}^{\mathrm{T}}\right)^{\mathrm{T}} \tag{10}$$

$$\hat{H}(\hat{\boldsymbol{Q}}, \hat{\boldsymbol{P}}) = K(\boldsymbol{Q}, \boldsymbol{P}, t) + \hat{P}_0 = 0. \tag{11}$$

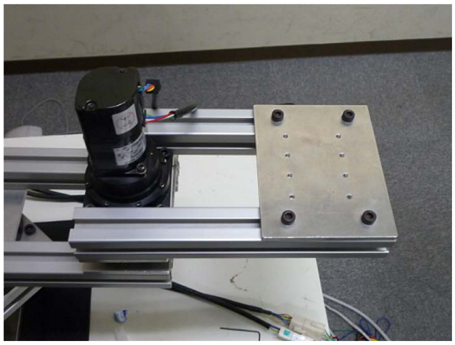

Fig. 1. Handle robot.

Fig. 2. Mobile robot.

The motion equation is transformed as follows:

$$\dot{\boldsymbol{x}} = \frac{\partial \boldsymbol{\Phi}}{\partial \boldsymbol{x}}\frac{d\boldsymbol{x}}{dt} = \frac{\partial \boldsymbol{\Phi}}{\partial \boldsymbol{x}}\left(\boldsymbol{J}\frac{\partial H(\boldsymbol{x})}{\partial \boldsymbol{x}}^{\mathrm{T}} + \boldsymbol{u}\right) \tag{12}$$

$$= \frac{\partial \boldsymbol{\Phi}}{\partial \boldsymbol{x}}\boldsymbol{J}\frac{\partial \boldsymbol{\Phi}}{\partial \boldsymbol{x}}^{\mathrm{T}}\frac{\partial H(\overline{\boldsymbol{x}})}{\partial \overline{\boldsymbol{x}}}^{\mathrm{T}} + \frac{\partial \boldsymbol{\Phi}}{\partial \boldsymbol{x}}\boldsymbol{u} \tag{13}$$

$$= \overline{\boldsymbol{J}}\frac{\partial H(\overline{\boldsymbol{x}})}{\partial \overline{\boldsymbol{x}}}^{\mathrm{T}} + \overline{\boldsymbol{u}}. \tag{14}$$

Here, $\bar{\boldsymbol{J}}$ and $\bar{\boldsymbol{u}}$ are defined as follows:

$$\overline{\boldsymbol{J}} = \frac{\partial \boldsymbol{\Phi}}{\partial \boldsymbol{x}}\boldsymbol{J}\frac{\partial \boldsymbol{\Phi}}{\partial \boldsymbol{x}}^{\mathrm{T}} \tag{15}$$

$$\overline{\boldsymbol{u}} = \frac{\partial \boldsymbol{\Phi}}{\partial \boldsymbol{x}}\boldsymbol{u}. \tag{16}$$

III. Mobile-Hapto

In this section, the dynamics and controller of mobile-hapto are derived.

A. Robots

Hamiltonian of robot systems is given as follows:

$$H = \frac{1}{2}\boldsymbol{p}^{\mathrm{T}}\boldsymbol{m}^{-1}\boldsymbol{p} \tag{17}$$

$$\hat{H} = H + p_0. \tag{18}$$

Here, $\boldsymbol{m}$ is a generalized mass matrix, and momentum $\boldsymbol{p}$ is given as follows:

$$\boldsymbol{p} = \boldsymbol{m}\dot{\boldsymbol{q}}. \tag{19}$$

In mobile-hapto, bilateral control is realized between a handle (local) robot and a mobile (remote) robot [27]. Fig. 1 shows the handle robot, and Fig. 2 shows the mobile robot. Fig. 3 shows a schematic of mobile-hapto. The velocity of the mobile robot is controlled by an operator, while the reaction force of the mobile robot is fed back to the operator. Then, the operator can recognize the environmental conditions of the mobile robot side. Variables q and f are position and force, respectively. Variables with subscripts 1 and 2 refer to the handle robot and the mobile robot, respectively. The inertia of the handle robot is m_1, and the mass of the mobile robot is m_2. The handle robot has a single DOF, and the mobile robot has two DOFs.

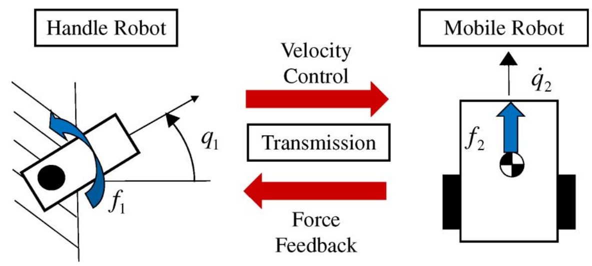

Fig. 3. Mobile-hapto.

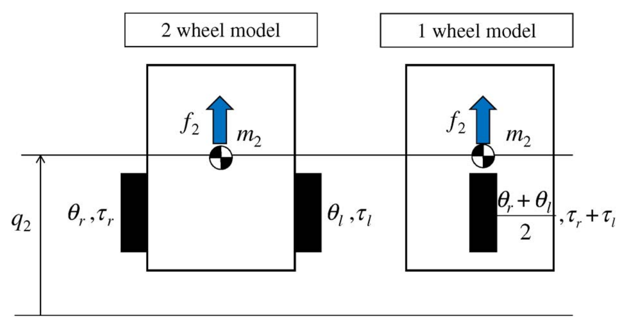

Fig. 4. Mobile robot model.

In this paper, we treated the mobile robot as a single-DOF system modeled in Fig. 4. θ_r, θ_l, τ_r, and τ_l are the angler positions and torques of the slave actuators, respectively. Therefore, there exist relations $q_2 = R((\theta_r + \theta_l)/2)$ and $f_2 = (\tau_r + \tau_l)/R$ with the radius of wheels denoted as R.

The dynamics of the system is parameterized by the proposed motion equation as follows:

$$\boldsymbol{x} = \begin{bmatrix} t \\ q_1 \\ q_2 \\ -H \\ p_1 \\ p_2 \end{bmatrix}, \quad \boldsymbol{u} = \begin{bmatrix} 0 \\ 0 \\ 0 \\ -f_1\frac{p_1}{m_1} - f_2\frac{p_2}{m_2} \\ f_1 \\ f_2 \end{bmatrix} \tag{20}$$

$$\boldsymbol{m} = \begin{bmatrix} m_1 & 0 \\ 0 & m_2 \end{bmatrix}, \quad \boldsymbol{J} = \begin{bmatrix} \boldsymbol{0} & \boldsymbol{I_3} \\ -\boldsymbol{I_3} & \boldsymbol{0} \end{bmatrix}. \tag{21}$$

B. Dynamics of Mobile-Hapto

In mobile-hapto, the velocity of the mobile robot is controlled by the inclination of the handle robot. At the same time, the reaction force of the mobile robot is fed back to the handle robot realizing the law of action and reaction. These two tasks are numerically given as follows:

$$q_1 - \alpha \dot{q}_2 = 0 \tag{22}$$
$$f_1 + \beta f_2 = 0 \tag{23}$$

where α and β are scaling gains. Note that (22) includes a velocity dimension value $\dot{q}_2$. The dynamics of mobile-hapto can be derived only by the proposed motion equation.

The phase variables (coordinate systems) are transformed to describe the dynamics of mobile-hapto as follows:

$$\overline{\boldsymbol{x}} = \begin{bmatrix} t \\ q_1 \\ q_2 \\ -H \\ q_1 - \alpha \dot{q}_2 \\ p_1 + \beta p_2 \end{bmatrix} = \begin{bmatrix} t \\ q_1 \\ q_2 \\ -H \\ q_1 - \frac{\alpha}{m_2} p_2 \\ p_1 + \beta p_2 \end{bmatrix}. \tag{24}$$

Substituting this equation for (14), the dynamics of mobile-hapto is revealed as follows:

$$\frac{d}{dt}\boldsymbol{Q}^{\mathrm{res}} = \boldsymbol{F}^{\mathrm{dis}} + \boldsymbol{F}^{\mathrm{ref}} - \boldsymbol{F}^{\mathrm{res}} \tag{25}$$
$$\boldsymbol{Q} = \begin{bmatrix} Q_1 \\ Q_2 \end{bmatrix} = \begin{bmatrix} q_1 - \frac{\alpha}{m_2} p_2 \\ p_1 + \beta p_2 \end{bmatrix} \tag{26}$$
$$\boldsymbol{F}^{\mathrm{dis}} = \begin{bmatrix} \frac{1}{m_1} p_1 \\ 0 \end{bmatrix}, \quad \boldsymbol{F}^{\mathrm{ref}} = \boldsymbol{T} \begin{bmatrix} f_1^{\mathrm{ref}} \\ f_2^{\mathrm{ref}} \end{bmatrix} \tag{27}$$
$$\boldsymbol{F}^{\mathrm{res}} = \begin{bmatrix} F_1^{\mathrm{res}} \\ F_2^{\mathrm{res}} \end{bmatrix} = \boldsymbol{T} \begin{bmatrix} f_1^{\mathrm{res}} \\ f_2^{\mathrm{res}} \end{bmatrix} \tag{28}$$
$$\boldsymbol{T} = \begin{bmatrix} 0 & -\frac{\alpha}{m_2} \\ 1 & \beta \end{bmatrix}. \tag{29}$$

Variables with superscripts *res* and *ref* stand for response and reference values, respectively. $\boldsymbol{F}^{\mathrm{dis}}$ is an interference term. Detailed derivation of the dynamics is written in the literature [26].

C. Implementation of Controller

Because mobile-hapto is a first-order time-derivative system as shown in (25), proportional position and force controllers are implemented

$$\boldsymbol{F}^{\mathrm{ref}} = \begin{bmatrix} -K_p Q_1^{\mathrm{res}} \\ -K_f F_2^{\mathrm{res}} \end{bmatrix} - \boldsymbol{F}^{\mathrm{cmp}} \tag{30}$$
$$= -\boldsymbol{S} K_p \boldsymbol{Q}^{\mathrm{res}} - (\boldsymbol{I_2} - \boldsymbol{S}) K_f \boldsymbol{F}^{\mathrm{res}} - \boldsymbol{F}^{\mathrm{cmp}} \tag{31}$$
$$\boldsymbol{F}^{\mathrm{cmp}} = \boldsymbol{F}^{\mathrm{dis}} \tag{32}$$

where K_p and K_f are feedback gains. $\boldsymbol{S}$ is a coordinate selection matrix defined as

$$\boldsymbol{S} = \begin{bmatrix} 1 & 0 \\ 0 & 0 \end{bmatrix}. \tag{33}$$

Therefore, the force references of robots f_1^{ref} and f_2^{ref} are derived as follows:

$$\boldsymbol{f}^{\mathrm{ref}} = \begin{bmatrix} f_1^{\mathrm{ref}} \\ f_2^{\mathrm{ref}} \end{bmatrix} = \boldsymbol{T}^{-1} \boldsymbol{F}^{\mathrm{ref}}. \tag{34}$$

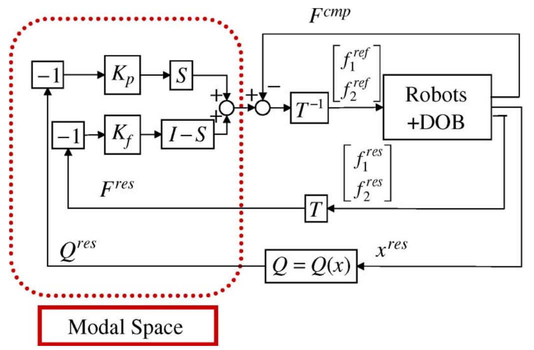

Fig. 5. Proposed mobile-hapto controller.

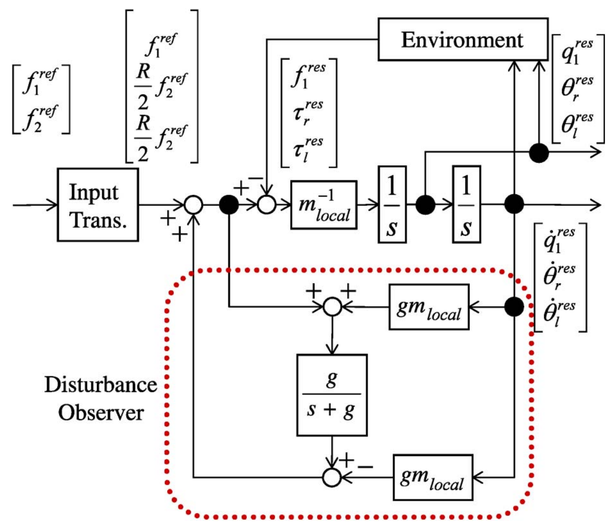

Fig. 6. Robot and DOB.

The torque references for wheels of the mobile robot are given as follows:

$$\tau_r = \tau_l = \frac{R}{2} f_2^{\mathrm{ref}}. \tag{35}$$

A DOB is implemented to reject disturbance forces. A block diagram of the control system is shown in Fig. 5. Details of "Robots + DOB" in Fig. 5 are shown in Fig. 6. First, the input is transformed from the force reference of the mobile robot to the torque reference of each wheel by using (35). Then, the DOB is composed using the mass matrix $\boldsymbol{m}_{\mathrm{local}}$, which includes the inertia of the handle robot and wheels and is defined as follows:

$$\boldsymbol{m}_{\mathrm{local}} = \begin{bmatrix} m_1 & 0 & 0 \\ 0 & \frac{R^2 m_2}{2} & 0 \\ 0 & 0 & \frac{R^2 m_2}{2} \end{bmatrix}. \tag{36}$$

As long as the yaw rate is negligibly small (i.e., $\dot{\theta}_r = \dot{\theta}_l$), the relation of kinetic energy

$$\frac{1}{2}\begin{bmatrix} \dot{q}_1 \\ \dot{q}_2 \end{bmatrix}^{\mathrm{T}} \boldsymbol{m} \begin{bmatrix} \dot{q}_1 \\ \dot{q}_2 \end{bmatrix} = \frac{1}{2}\begin{bmatrix} \dot{q}_1 \\ \dot{\theta}_r \\ \dot{\theta}_l \end{bmatrix}^{\mathrm{T}} \boldsymbol{m}_{local} \begin{bmatrix} \dot{q}_1 \\ \dot{\theta}_r \\ \dot{\theta}_l \end{bmatrix} \tag{37}$$

holds.

IV. Analysis

In this section, first, the conventional and proposed methods are analyzed. Then, the robustness of the proposed method is analyzed.

A. Conventional Method

Here, the conventional method [27] is analyzed. Force references of the conventional method $\boldsymbol{f}_{\text{con}}^{\text{ref}}$ are given as follows:

$$\boldsymbol{f}_{\text{con}}^{\text{ref}} = \begin{bmatrix} \frac{m_1}{2\alpha}\left(-C_p Q_1^{\text{res}} - C_f F_2^{\text{res}}\right) \\ \frac{m_2}{2s}\left(C_p Q_1^{\text{res}} - C_f F_2^{\text{res}}\right) \end{bmatrix} \tag{38}$$

$$C_p = K_p + K_v s \tag{39}$$

$$C_f = K_f. \tag{40}$$

In the conventional method, position control is specified by a proportional–derivative controller C_p. The parameter K_v is velocity feedback gain. Substituting (38) for (25), the responses in the Laplace frequency domain are derived as follows:

$$\begin{bmatrix} \frac{\alpha K_p + \alpha K_v s + 2s^2}{2s} & 0 \\ \frac{(m_1 s - m_2\alpha\beta)(K_p + K_v s)}{2\alpha s} & s \end{bmatrix} \boldsymbol{Q}^{\text{res}} = \begin{bmatrix} -1 & \frac{\alpha K_f}{2s} \\ 0 & \frac{-m_1 K_f s - m_2 K_f \alpha\beta - 2\alpha s}{2\alpha s} \end{bmatrix} \boldsymbol{F}^{\text{res}} + \begin{bmatrix} s q_1^{\text{res}} \\ 0 \end{bmatrix}. \tag{41}$$

Therefore, the following matrix $\boldsymbol{A}$ describes the dynamic behavior:

$$\boldsymbol{A} = \begin{bmatrix} -1 & \frac{\alpha K_f}{2s} \\ 0 & \frac{-m_1 K_f s - m_2 K_f \alpha\beta - 2\alpha s}{2\alpha s} \end{bmatrix}^{-1} \times \begin{bmatrix} \frac{\alpha K_p + \alpha K_v s + 2s^2}{2s} & 0 \\ \frac{(m_1 s - m_2\alpha\beta)(K_p + K_v s)}{2\alpha s} & s \end{bmatrix}. \tag{42}$$

Obviously, $\boldsymbol{A}$ is not a diagonal matrix. Owing to the off-diagonal parameters of $\boldsymbol{A}$, the position and force tasks interfere each other. In addition, because the characteristic polynomial of $\boldsymbol{A}$ is third order, the system has a possibility to be unstable. Hence, it is difficult to design stable and precise mobile-hapto control in the conventional method.

B. Proposed Method

The responses in the proposed method are analyzed by substituting (30) for (25)

$$Q_1^{\text{res}} = -\frac{F_1^{\text{res}}}{K_p + s} \tag{43}$$

$$F_2^{\text{res}} = -\frac{s Q_2^{\text{res}}}{1 + K_f}. \tag{44}$$

Because the tasks are defined as coordinate transform, there are no interferences of the tasks. The two tasks can be designed as a combination of two single-DOF tasks. Thus, the performance of mobile-hapto can be improved by the proposed method. Equations (43) and (44) clearly show that the responses in the proposed method are stable.

TABLE I
PARAMETERS

m_1	Inertia (Handle robot)	0.015 [kgm^2]
m_2	Mass (Mobile robot)	8.64 [kg]
R	Wheel Radius	0.075 [m]
K_f	Force Feedback Gain	1.0
K_p	Proportional Gain	100 [1/s^2]
K_v	Differential Gain (conventional)	16 [1/s]
α	Scaling Gain (Position)	0.2
β	Scaling Gain (Force)	0.04
g	Cut-off Angular Frequency of DOB	50 [rad/s]
g_r	Cut-off Angular Frequency of RFOB	50 [rad/s]
g_p	Cut-off Angular Frequency of Pseudo Differential	50 [rad/s]
St	Sampling Time	0.0001 [s]

C. Robustness

The effect of modeling errors of $\boldsymbol{T}$ is analyzed here.

$$\boldsymbol{T}_n + \Delta\boldsymbol{T} = \boldsymbol{T} \tag{45}$$

where $\boldsymbol{T}_n$ is a nominal matrix of $\boldsymbol{T}$ and $\Delta\boldsymbol{T}$ is its modeling error. They can be rewritten by a nominal mass of the mobile robot m_{2n} and its modeling error Δm_2

$$\boldsymbol{T}_n = \begin{bmatrix} 0 & -\frac{\alpha}{m_{2n}} \\ 1 & \beta \end{bmatrix} \tag{46}$$

$$\Delta\boldsymbol{T} = \begin{bmatrix} 0 & \frac{\alpha\Delta m_2}{m_2 m_{2n}} \\ 1 & \beta \end{bmatrix}. \tag{47}$$

Therefore, the force references are calculated by (48) in the presence of modeling errors

$$\boldsymbol{f}_n^{\text{ref}} = \boldsymbol{T}_n^{-1}\left(\begin{bmatrix} -K_p Q_1^{\text{res}} \\ -K_f F_2^{\text{res}} \end{bmatrix} - \begin{bmatrix} \dot{q}_1 \\ 0 \end{bmatrix}\right). \tag{48}$$

The reference $\boldsymbol{f}_n^{\text{ref}}$ is a force reference including modeling errors. The dynamics of the mobile-hapto is derived by (25), (29), and (48)

$$\frac{d}{dt}\boldsymbol{Q}^{\text{res}} = \begin{bmatrix} \dot{q}_1 \\ 0 \end{bmatrix} + \boldsymbol{T}\boldsymbol{f}_n^{\text{ref}} - \boldsymbol{F}^{\text{res}} \tag{49}$$

$$= \begin{bmatrix} \frac{\Delta m_2}{m_2}\dot{q}_1 \\ 0 \end{bmatrix} - \begin{bmatrix} \frac{m_{2n}}{m_2} K_p Q_1^{\text{res}} \\ K_f F_2^{\text{res}} \end{bmatrix} - \boldsymbol{F}^{\text{res}}. \tag{50}$$

This equation shows that the force transmission task is not deteriorated by the modeling error of m_2. The first row of (50) is rewritten as follows:

$$Q_1^{\text{res}} = \frac{\frac{\Delta m_2}{m_2} s q_1 - F_1^{\text{res}}}{\frac{m_{2n}}{m_2} K_p + s}. \tag{51}$$

Even though the modeling error deteriorates the response, the velocity control task is still a stable first-order system.

V. Experiment

In this section, the validity of the proposed method is experimentally verified. Here, we assume that the wheels do not slip and yaw rate control of the mobile robot was neglected because the floor used in this experiment has sufficient friction coefficients. The yaw rate control of mobile-hapto was discussed in the literature [28]. The reaction forces of the robots were estimated by a reaction force observer (RFOB) [29]. Table I exhibits the control parameters of the experiment.

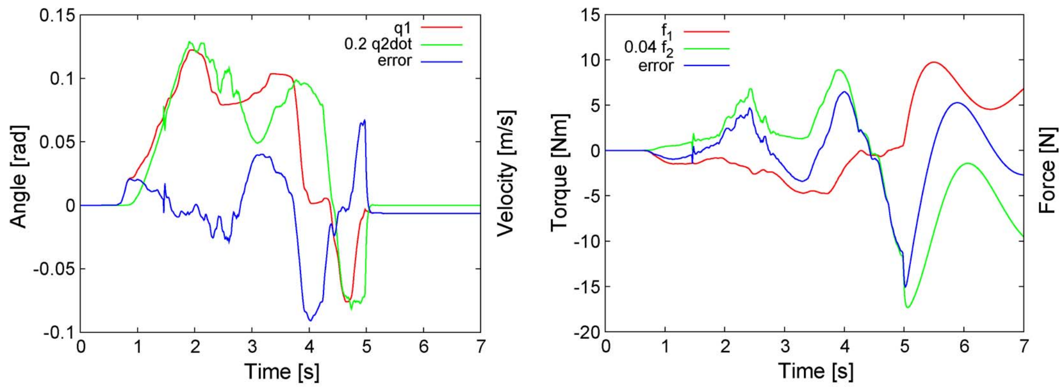

(a) (b)

Fig. 7. Experimental results (conventional method). (a) Position response. (b) Force response.

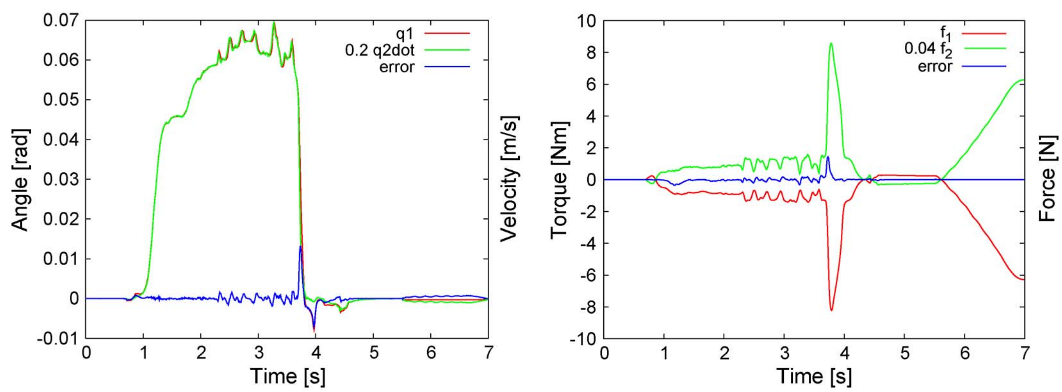

(a) (b)

Fig. 8. Experimental results (proposed method, $m_{2n} = m_2$). (a) Position response. (b) Force response.

A. Experiment 1: Performance Comparison Experiment

In this experiment, the performances of the conventional method and the proposed method were compared. Figs. 7 and 8 show experimental results of the conventional method and that of the proposed method, respectively. Part (a) shows the position response of the handle robot and the velocity response of the mobile robot. Part (b) displays the torque response of the handle robot and the force response of the mobile robot. The red, green, and blue lines are responses of the handle robot, that of the mobile robot, and the errors, respectively. The motion of the mobile robot was categorized in three phases. First, the mobile robot freely moved (0–2.5 s). Then, the mobile robot traveled through a rough terrain (2.5–3.8 s). Finally, the mobile robot contacted a wall and pushed it (3.8–7 s). Because the handle robot was manipulated by an operator, the trajectories of the handle were similar but not completely equal.

Fig. 7(a) shows that there were large errors between the inclination of the handle robot and the velocity of the mobile robot, while Fig. 7(b) shows that it was difficult for the operator to feel the reaction force of the environment. Fig. 8(a) shows that the velocity of the mobile robot well matched the inclination of the handle robot, while Fig. 8(b) shows that the law of action and reaction was precisely established between the handle and mobile robots. The operator could manipulate the velocity of the mobile robot feeling the reaction force. Namely, the operator could distinguish the environmental conditions by the reaction force during the driving. Therefore, these experimental results clearly demonstrated that the proposed method is superior over the conventional method. Because the dynamics of mobile-hapto is not derived in the conventional method, the interference among the handle robot, the mobile robot, the position controller, and the force controller deteriorated the performance. By contrast, because the proposed method is derived based on the dynamics of mobile-hapto, which can be derived only by the proposed motion equation, precise and stable mobile-hapto responses were obtained.

B. Experiment 2: Robustness Verification Experiment

In this experiment, the effect of the modeling errors was demonstrated. To verify the robustness of the proposed method against parameter variation of m_2, we changed the nominal value of the mobile robot m_{2n}. Figs. 9 and 10 show the experimental results of the proposed method with modeling errors ($m_{2n} = 0.2m_2$ and $m_{2n} = 5m_2$). We see that the control performance is still satisfactory with respect to the position and velocity accordance and the realization of the law of action and reaction. The robots were hardly influenced by the modeling errors in the proposed method. As it was discussed in Section IV, owing to the dynamics, which is a first-order system, the proposed controller is robust against the parameter variation.

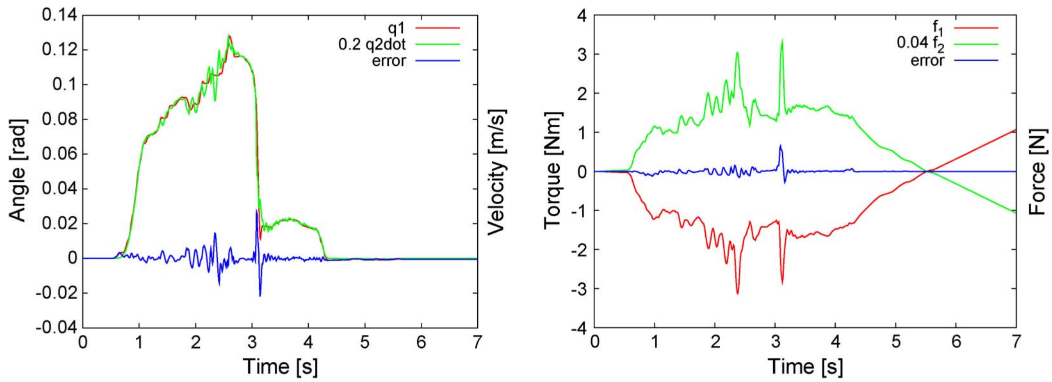

(a) (b)

Fig. 9. Experimental results (proposed method, $m_{2n} = 0.2m_2$). (a) Position response. (b) Force response.

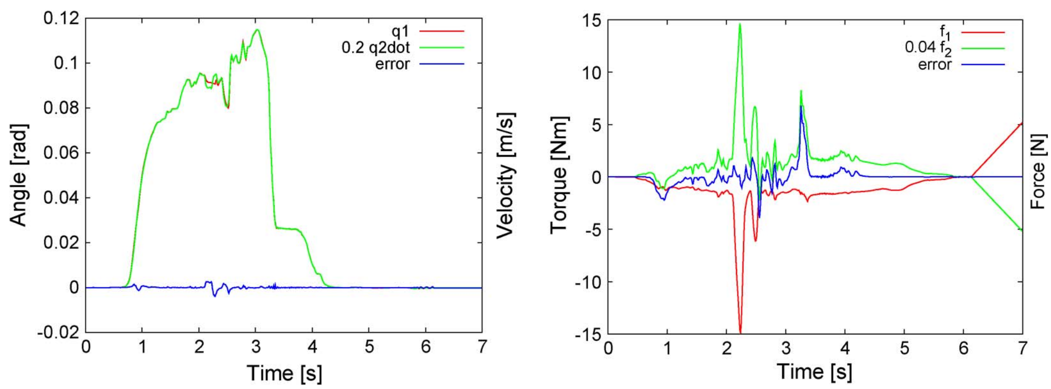

(a) (b)

Fig. 10. Experimental results (proposed method, $m_{2n} = 5m_2$). (a) Position response. (b) Force response.

TABLE II
ABSOLUTE POSITION ERROR

	Position Error [rad]	
	Maximum	Mean
Conventional	9.10×10^{-2}	1.68×10^{-2}
Proposed ($m_{2n} = m_2$)	1.32×10^{-2}	5.17×10^{-4}
Proposed ($m_{2n} = 0.2m_2$)	2.68×10^{-2}	1.36×10^{-3}
Proposed ($m_{2n} = 5m_2$)	3.96×10^{-3}	2.21×10^{-4}

TABLE III
ABSOLUTE FORCE ERROR

	Force Error [Nm]	
	Maximum	Mean
Conventional	1.50×10	2.64
Proposed ($m_{2n} = m_2$)	1.44	4.80×10^{-2}
Proposed ($m_{2n} = 0.2m_2$)	6.16×10^{-1}	2.40×10^{-2}
Proposed ($m_{2n} = 5m_2$)	6.79	3.55×10^{-1}

C. Discussion

Tables II and III exhibit the maximum and mean absolute errors of the position and force responses, respectively. The tables clearly show that the control accuracy of the proposed method was far better than that of the conventional method. We see the minimum position errors in the proposed method $(m_{2n} = 5m_2)$, because, as it can be understood from (51), the position feedback gain K_p was substituted for higher feedback gain $[(m_{2n}/m_2)K_p = 5K_p]$. However, the experiment [proposed $(m_{2n} = 5m_2)$] showed the maximum force errors in the three experiments of the proposed method. Because the reaction forces were estimated by the RFOB, the estimation error was increased by the modeling error Δm_2. Hence, the force regulation performance was degraded with the largest modeling error ($\Delta m_2 = 4m_2$ with $m_{2n} = 5m_2$). We see few differences in the responses of the other proposed methods. It is caused by the difference of the trajectories given by the operator.

The mobile robot experienced three phases: free-moving phase, rough-terrain phase, and wall-pushing phase. However, there were small dependences on the phases since the DOB increased the robustness to environmental conditions. Then, we can summarize that the proposed system can be applied to the real systems.

VI. CONCLUSION

In this paper, the dynamics of mobile-hapto has been revealed using the previous study's proposed motion equation, and the conventional and proposed mobile-hapto controllers were analyzed using the dynamics. We showed that tasks can be independently designed only in the proposed method because arbitrary tasks can be treated as coordinate transform by the proposed motion equation. The proposed mobile-hapto controller, which is a proportional controller, is stable since we revealed that mobile-hapto systems are first-order time-derivative systems. Furthermore, the proposed method showed strong robustness. The experimental results showed the effectiveness of the proposed controller. With the proposed approach, designers are not hindered by interferences of tasks. Once a stable and precise controller is created, it can be reused in other systems with less effort.

REFERENCES

[1] K. Ohnishi, M. Shibata, and T. Murakami, "Motion control for advanced mechatronics," *IEEE/ASME Trans. Mechatronics*, vol. 1, no. 1, pp. 56–67, Mar. 1996.

[2] C. W. Lee and C. C. Chung, "Design of a new multi-loop disturbance observer for optical disk drive systems," *IEEE Trans. Magn.*, vol. 45, no. 5, pp. 2224–2227, May 2009.

[3] K.-S. Kim, K.-H. Rew, and S. Kim, "Disturbance observer for estimating higher order disturbances in time series expansion," *IEEE Trans. Autom. Control*, vol. 55, no. 8, pp. 1905–1911, Aug. 2010.

[4] Q. W. Jia, "Disturbance rejection through disturbance observer with adaptive frequency estimation," *IEEE Trans. Magn.*, vol. 45, no. 6, pp. 2675–2678, Jun. 2009.

[5] K. Kaneko, K. Komoriya, and K. Tanie, "Operational space manipulator control based on variable disturbance observer," in *Proc. IEEE Int. Workshop Adv. Motion Control*, 1993, pp. 623–630.

[6] K. Natori, T. Tuji, and K. Ohnishi, "Time-delay compensation by communication disturbance observer for bilateral teleoperation under time-varying delay," *IEEE Trans. Ind. Electron.*, vol. 57, no. 3, pp. 1050–1062, Mar. 2010.

[7] J. Yi, S. Chang, and Y. Shen, "Disturbance-observer-based hysteresis compensation for piezoelectric actuators," *IEEE/ASME Trans. Mechatronics*, vol. 14, no. 4, pp. 456–464, Aug. 2009.

[8] K. Abidi and A. Sabanovic, "Sliding-mode control for high-precision motion of a piezostage," *IEEE Trans. Ind. Electron.*, vol. 54, no. 1, pp. 629–637, Feb. 2007.

[9] Y.-S. Lu, "Sliding-mode disturbance observer with switching-gain adaptation and its application to optical disk drives," *IEEE Trans. Ind. Electron.*, vol. 56, no. 9, pp. 3743–3750, Sep. 2009.

[10] B. K. Kim, W. K. Chung, and K. Ohba, "Design and performance tuning of sliding-mode controller for high-speed and high-accuracy positioning systems in disturbance observer framework," *IEEE Trans. Ind. Electron.*, vol. 56, no. 10, pp. 3798–3809, Oct. 2009.

[11] S. Oh, T. Koyanagi, and Y. Hori, "Force sensor-less assist control design based on two-degree-of-freedom control," in *Proc. ICCAS-SICE*, 2009, pp. 1633–1638.

[12] R. A. Brooks, "A robust layered control system for a mobile robot," *IEEE J. Robot. Autom.*, vol. RA-2, no. 1, pp. 14–23, Mar. 1986.

[13] M. Cossentino, L. Sabatucci, and A. Chella, "A possible approach to the development of robotic multi-agent systems," in *Proc. IEEE/WIC Int. Conf. Intell. Agent Technol.*, 2003, pp. 539–544.

[14] T. Tsuji, K. Ohnishi, and A. Sabanovic, "A controller design method based on functionality," *IEEE Trans. Ind. Electron.*, vol. 54, no. 6, pp. 3335–3343, Dec. 2007.

[15] A. Sabanovic, M. Elitas, and K. Ohnishi, "Sliding modes in constrained systems control," *IEEE Trans. Ind. Electron.*, vol. 55, no. 9, pp. 3332–3339, Sep. 2008.

[16] S. Sakaino, T. Sato, and K. Ohnishi, "Multi-DOF micro macro bilateral controller using oblique coordinate control," *IEEE Trans. Ind. Informat.*, vol. 7, no. 3, pp. 446–454, Aug. 2011.

[17] J. Y. S. Luh, M. W. Walker, and R. P. C. Paul, "Resolved-acceleration control of mechanical manipulators," *IEEE Trans. Autom. Control*, vol. AC-28, no. 3, pp. 468–474, Jun. 1980.

[18] O. Khatib, "A unified approach for motion and force control of robot manipulators: The operational space formulation," *IEEE Trans. Robot. Autom.*, vol. RA-3, no. 1, pp. 43–53, Feb. 1987.

[19] R. Featherstone and O. Khatib, "Load independence of the dynamically consistent inverse of the Jacobian matrix," *Int. J. Robot. Res.*, vol. 16, no. 2, pp. 168–170, Apr. 1997.

[20] K. Fujimoto and T. Sugie, "Canonical transformation and stabilization of generalized Hamiltonian systems," in *Proc. 4th IFAC Symp. Nonlinear Control Syst. Des.*, Jul. 1998, pp. 7–12.

[21] K. Fujimoto and T. Sugie, "Canonical transformation and stabilization of generalized Hamiltonian systems," *Syst. Control Lett.*, vol. 42, no. 3, pp. 217–227, Mar. 2001.

[22] A. J. van der Schaft and B. Maschke, "On the Hamiltonian formulation of nonholonomic mechanical systems," *Rep. Math. Phys.*, vol. 34, no. 2, pp. 225–233, Aug. 1994.

[23] R. Ortega, A. J. van der Schaft, and B. Maschke, "Interconnection and damping assignment passivity-based control of port-controlled Hamiltonian systems," *Automatica*, vol. 38, no. 4, pp. 585–596, Apr. 2002.

[24] K. Fujimoto, K. Sakurama, and T. Sugie, "Trajectory tracking control of port-controlled Hamiltonian systems via generalized canonical transformations," *Automatica*, vol. 39, no. 12, pp. 2059–2069, Dec. 2003.

[25] K. Fujimoto, K. Sakurama, and T. Sugie, "Trajectory tracking control of nonholonomic Hamiltonian systems via generalized canonical transformations," *Eur. J. Control*, vol. 10, no. 5, pp. 421–431, May 2004.

[26] S. Sakaino, T. Sato, and K. Ohnishi, "A novel motion equation for general task description," in *Proc. 11th IEEE AMC*, Mar. 2010, pp. 566–571.

[27] W. Yamanouchi, Y. Yokokura, S. Katsura, and K. Ohishi, "Bilateral teleoperation with dimensional scaling for realization of mobile-hapto," in *Proc. 34th Annu. Conf. IEEE Ind. Electron.*, Nov. 2008, pp. 1590–1595.

[28] S. Sakaino, T. Sato, and K. Ohnishi, "Mobile-hapto with yaw rate control for traveling on rough terrain," in *Proc. 36th Annu. Conf. IEEE Ind. Electron. Soc.*, Nov. 2010, pp. 1559–1564.

[29] T. Murakami, F. Yu, and K. Ohnishi, "Torque sensorless control in multidegree-of-freedom manipulator," *IEEE Trans. Ind. Electron.*, vol. 40, no. 2, pp. 259–265, Apr. 1993.

Sho Sakaino (S'07–M'11) received the B.E. degree in system design engineering and the M.E. and Ph.D. degrees in integrated design engineering from Keio University, Yokohama, Japan, in 2006, 2008, and 2011, respectively.

Since 2011, he has been with Sakaino Laboratory, Department of Electrical and Electronic Systems, Saitama University, Saitama, Japan. His research interests include mechatronics, motion control, robotics, and haptics.

Dr. Sakaino is the recipient of the Institute of Electrical Engineers of Japan Industry Application Society Distinguised Transaction Paper Award.

Tomoya Sato (S'08) was born in Fujisawa, Japan, in 1984. He received the B.E. degree in system design engineering and the M.E. and Ph.D. degrees in integrated design engineering from Keio University, Yokohama, Japan, in 2007, 2009, and 2010, respectively.

He is with Ohnishi Laboratory, Department of System Design Engineering, Keio University. His research interests include motion control of biped robots and haptics.

Kouhei Ohnishi (S'78–M'80–SM'00–F'01) received the B.E., M.E., and Ph.D. degrees in electrical engineering from the University of Tokyo, Tokyo, Japan, in 1975, 1977, and 1980, respectively.

Since 1980, he has been with Ohnishi Laboratory, Department of System Design Engineering, Keio University, Yokohama, Japan. His research interests include mechatronics, motion control, robotics, and haptics.

Dr. Ohnishi is the recipient of the Best Paper Awards from the Institute of Electrical Engineers of Japan and the Japan Society for Precision Engineering and the Outstanding Paper Awards at IEEE International Conference on Industrial Electronics, Control, and Instrumentation, 1985, IEEE International Conference on Industrial Electronics, Control, and Instrumentation, 1992, and IEEE International Conference on Industrial Electronics, Control, and Instrumentation, 1993. He is also the recipient of the International Power Electronics and Motion Control Conference Council Award and the Dr.-Ing. Eugene Mittelmann Achievement Award from the IEEE Industrial Electronics Society in 2004.